

**Wind variability and Earth's rotation as drivers of transport in a deep, elongated  
subalpine lake: The case of Lake Garda**

**Marina AMADORI,<sup>1\*</sup> Sebastiano PICCOLROAZ,<sup>2</sup> Lorenzo GIOVANNINI,<sup>1</sup>  
Dino ZARDI,<sup>1,3</sup> Marco TOFFOLON<sup>1</sup>**

<sup>1</sup>Department of Civil, Environmental and Mechanical Engineering (DICAM), University of Trento, Italy

<sup>2</sup>Institute for Marine and Atmospheric Research (IMAU), Department of Physics, Utrecht University, The Netherlands

<sup>3</sup>Center Agriculture Food Environment (C3A), University of Trento, Italy

\*Corresponding author: [marina.amadori@unitn.it](mailto:marina.amadori@unitn.it)

## IMPLEMENTATION OF THE ATMOSPHERIC MODEL

The WRF simulations performed for the present work covered 48 hours each. The first 24 hours are spin-up time, and were not taken into account for the analysis. The horizontal domain covered an area that includes Lake Garda and was composed of three two-way nested domains with 94x90, 112x97 and 73x106 cells, and grid spacing of 9, 3 and 1 km, respectively. For the vertical resolution, 30 levels were used. The initial and boundary conditions were supplied by the 6-hourly National Centers for Environmental Prediction (NCEP) Final Operational Global Analysis data on 1-degree grids. For the land use the Corine Land Cover dataset, with a spatial resolution of 100 m, was used, provided by the European Environment Agency (<http://www.eea.europa.eu>). This dataset was reclassified into the standard IGBP classes, in order to fit the WRF look-up tables.

Relevant variables for forcing the hydrodynamic model from the last domain (1 km spatial resolution) were saved every 15 minutes starting from the midnight (00:00 UTC+0) of the simulation day.

## IMPLEMENTATION OF THE HYDRODYNAMIC MODEL

In Tabs. S1 and S2 the main parameters of the hydrodynamic and Lagrangian models are respectively summarized.

**Drag coefficients:** A Chezy coefficient value of  $65 \text{ m}^{1/2}\text{s}^{-1}$  is applied uniformly for the whole lake as bottom shear stress is not relevant for wind-induced transport in a deep lake. The wind drag coefficient  $C_d$  is specified as a piece-wise function of wind speed  $W$  with values taken in accordance with Wüest and Lorke (2003): 0.0044 for  $W \leq 1 \text{ m s}^{-1}$ , 0.001 for  $1 \leq W < 20 \text{ m s}^{-1}$ , and 0.002 for higher wind speed. A linear interpolation is applied in between.

## LENGTH AND TIME SCALES

**Duration of the simulation:** The repetition of a windy day in adiabatic conditions leads to the de-stratification of the lake and consequently facilitates vertical entrainment of the underlying deep water, as long as wind mixing is not balanced by the heat source at the surface during the day. The results discussed in the main text are obtained from the third day of simulation, using two spin-up days for the establishment of periodic conditions on surface currents.

**Spin-up time:** In order to have consistent and representative time-averaged results (i.e., residual circulation), two days have been considered as necessary (and sufficient) for the establishment of

periodic conditions on surface currents (see also Section 2 in the main text). The estimate is mainly based on direct observation of the periodic patterns reproduced by the numerical results after the second day (not showed here). Choosing a longer spin-up time would have drawbacks: since thermal fluxes are neglected and the same daily wind pattern is repeated for consecutive days, preliminary simulations showed that destratification appears to be relevant after the fourth simulation day. Hence, the third day has been chosen as the characteristic period for hydrodynamic results. The Lagrangian simulations also start at the beginning of the third day and last for two days, ending with the fourth day. In such a way, regime conditions are achieved and thermal stratification is substantially preserved.

**Time scale of vertical diffusion of momentum:** The definition of a spin up time of two days also has a theoretical justification. Describing the vertical momentum transport as a diffusive process in a shear flow, the shear stress  $\tau_{xz}$  produced by the gradient of the horizontal  $x$ -velocity  $u$  along the vertical  $z$ -direction is evaluated assuming the usual Boussinesq closure:

$$\tau_{xz} = \rho v_z^T \frac{\partial u}{\partial z} \quad (1)$$

An equivalent relationship holds for  $\tau_{yz}$  in the other horizontal direction,  $y$ . Assuming that the wind shear is transmitted to the lower layers by means of turbulent viscosity, the vertical scale  $D_m$  of the turbulent momentum transport can be obtained from Equation (1):

$$D_m \simeq \frac{\rho v_z^T}{\tau_w} U_s \quad (2)$$

where all variables are averaged over characteristic time and spatial scales, and  $U_s$  is a reference value of the surface velocity magnitude. The time scale of the diffusion process can be defined as:

$$T \simeq \frac{D_m^2}{v_z^T} \quad (3)$$

In winter simulations characterized by Föhn winds, the mean wind speed  $W \sim 15 \text{ m s}^{-1}$  produces a shear stress  $\tau_w \sim 4 \times 10^{-1} \text{ Pa}$  and induces velocities  $U_s \sim 30 \text{ cm s}^{-1}$  at lake surface. Hence, the vertical scale of turbulent momentum transport is  $D_m \sim 100 \text{ m}$ , due to the high vertical eddy viscosity ( $v_z^T \sim 5 \times 10^{-2} \text{ m}^2 \text{ s}^{-1}$ ) produced by the strong wind intensity. In summer simulations, the shear stress is smaller ( $\tau_w \sim 4 \times 10^{-3} \text{ Pa}$ ) due to the lower wind intensity ( $W \sim 5 \text{ m s}^{-1}$ ). Additionally, the vertical eddy viscosity is negatively influenced by thermal stratification ( $v_z^T \sim 5 \times 10^{-4} \text{ m}^2 \text{ s}^{-1}$ ). Taking as a reference the thickness of the surface layer  $D_m$ , the values of 10 m

and 100 m for summer and winter simulations, respectively, and  $v_z^T$  as the values of the vertical eddy viscosities ( $\sim 5 \times 10^{-4} \text{ m}^2 \text{ s}^{-1}$  and  $5 \times 10^{-2} \text{ m}^2 \text{ s}^{-1}$  respectively), the resulting time scale is of the order of two days in both cases.

### **LAGRANGIAN PARTICLE TRACKING MODEL**

All Lagrangian particles are released at the beginning of the third day (00:00) of the hydrodynamic simulation.

If the release starts at a different time (i.e., 6, 12, or 18 hours later), the wind forcing can initially move the Lagrangian drifters in a opposite direction, but the final pattern of the released particles does not significantly differ from the results obtained (Fig. S13), especially inside the largest gyres. In other words, even though diurnal fluctuation of wind direction influences the instantaneous water transport, particles tracks reflect the mean flow field: inside the gyre structures, daily periodical trajectories develop, suggesting that instantaneous velocities are essentially driven by the alternating wind direction. Inertial trajectories are drawn in the southern part, where residual velocities are lower, but only where Rossby radii are smaller than the dimensions of the lake. Lagrangian trajectories were obtained neglecting diffusive processes in the particle tracking simulations. Such a simplification was necessary as additional calibration parameters would be needed to adequately compute the dispersion parameters in Delft3D-Part, and calibration is not yet possible at this stage.

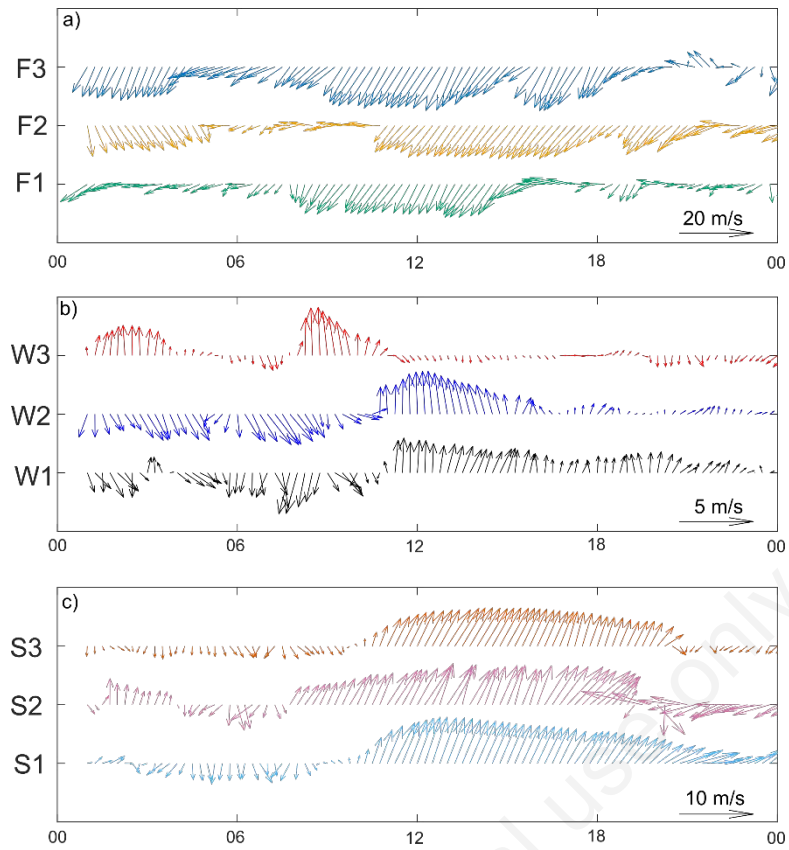


**Fig. S1.** Diurnal wind cycles at 10 m above ground level for winter Föhn days (a), winter breeze days (b) and summer (c) breeze days in the APPA monitoring point. Time given in UTC+1 (local time zone).

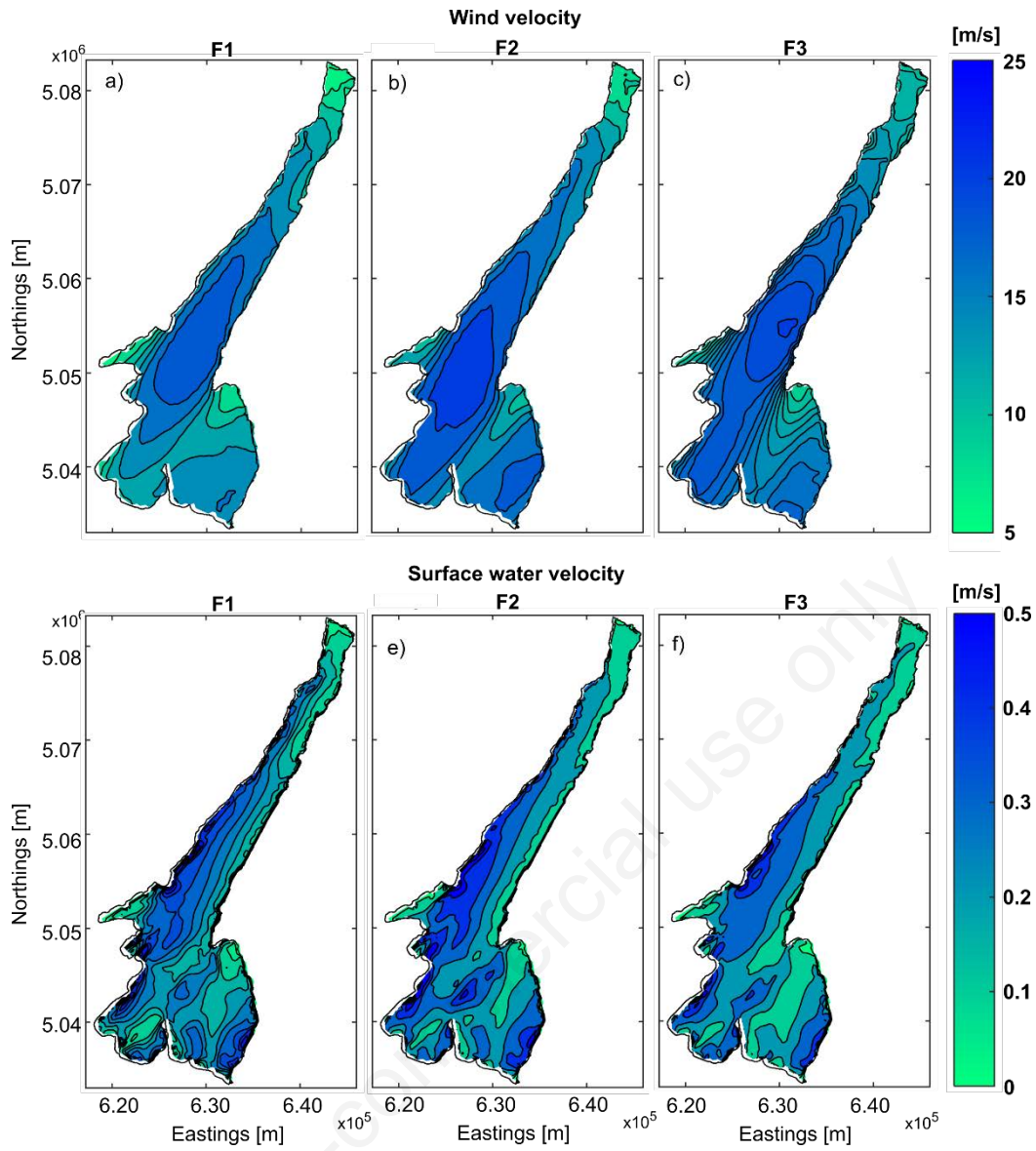


**Fig. S2.** Mean wind (top plots) and surface current intensities (bottom plots) in winter Föhn simulations.

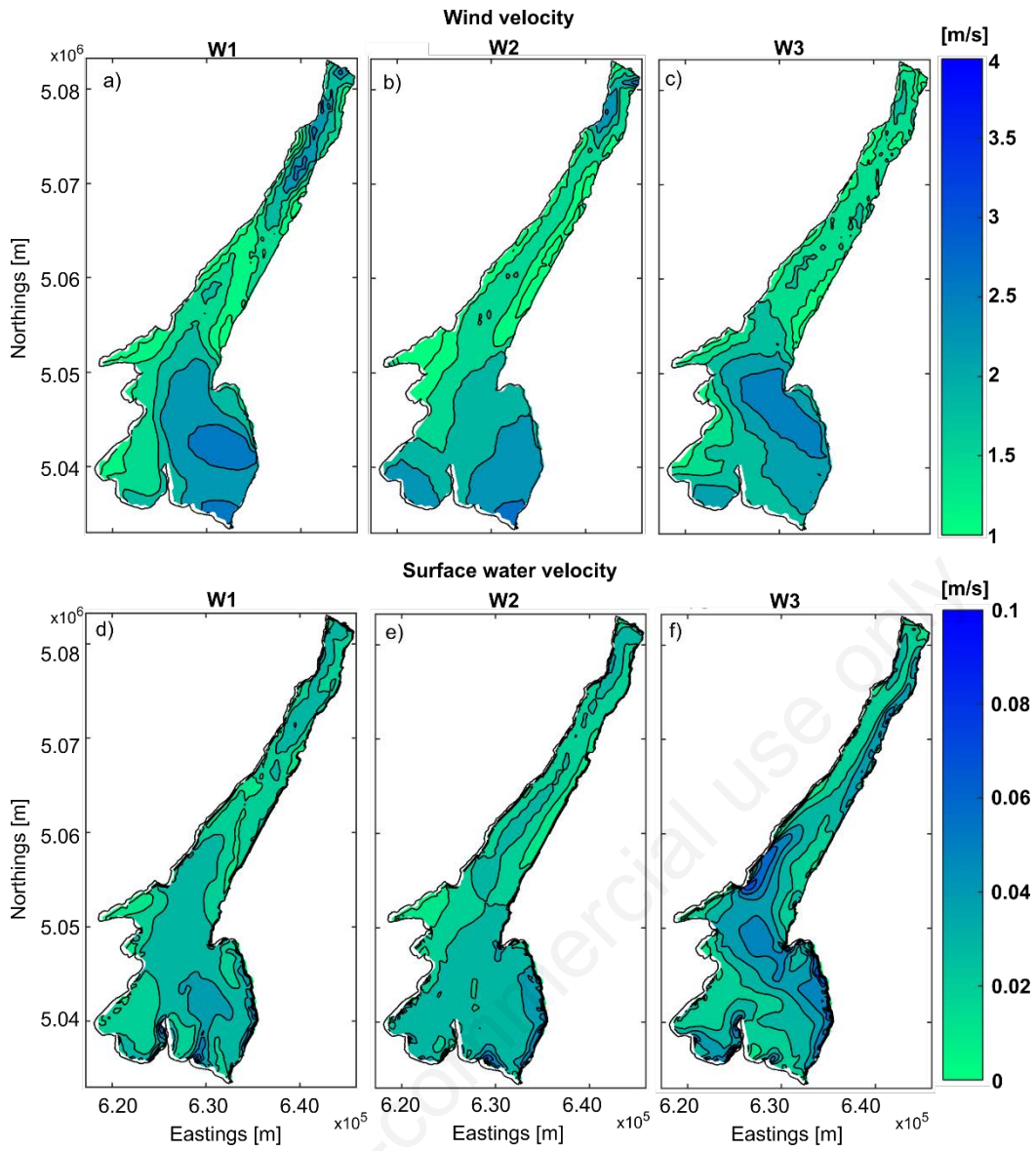


**Fig. S3.** Mean wind (top plots) and surface current intensities (bottom plots) in winter ordinary breeze simulations.

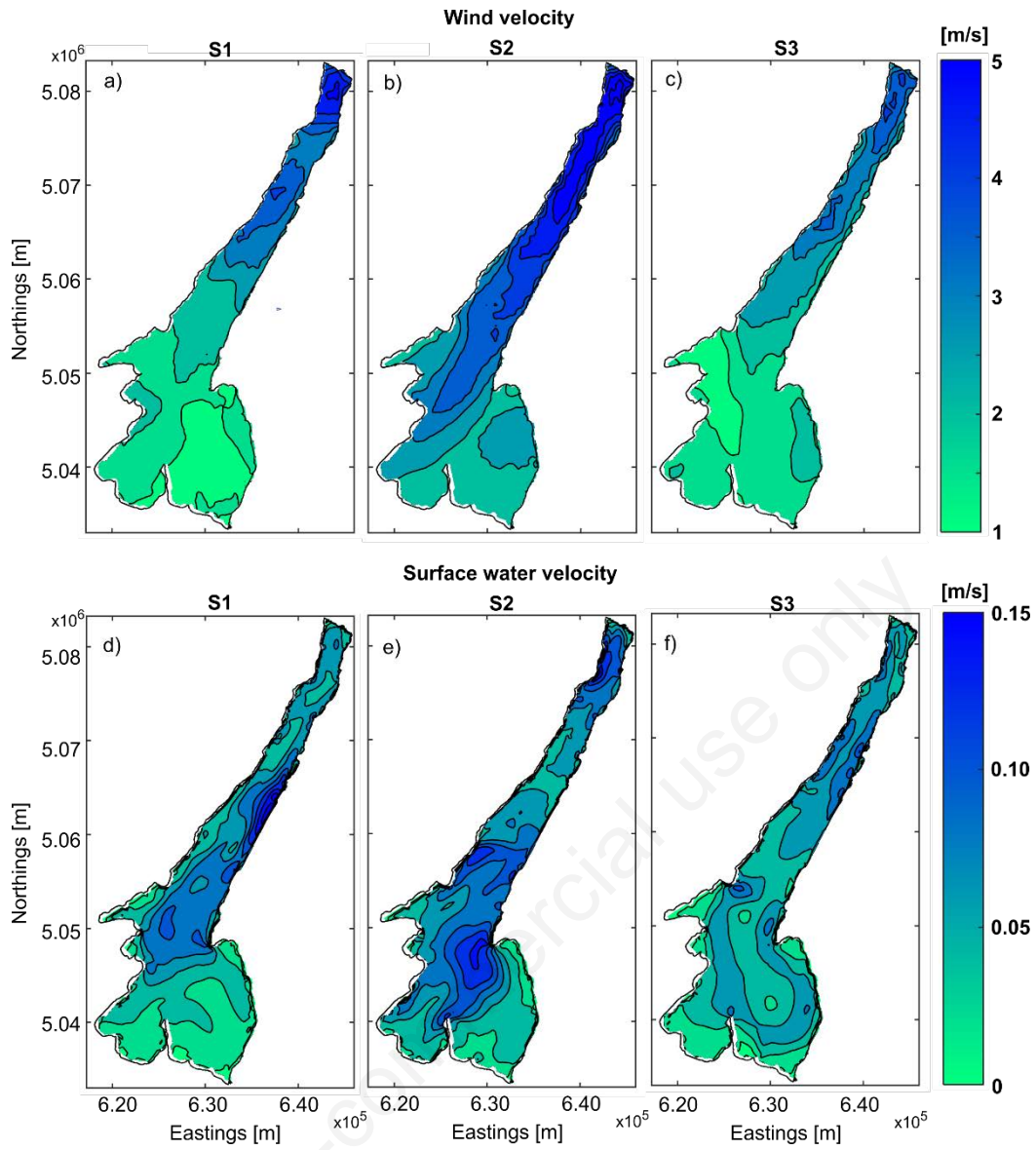


**Fig. S4.** Mean wind (top plots) and surface current intensities (bottom plots) in summer breeze simulations.



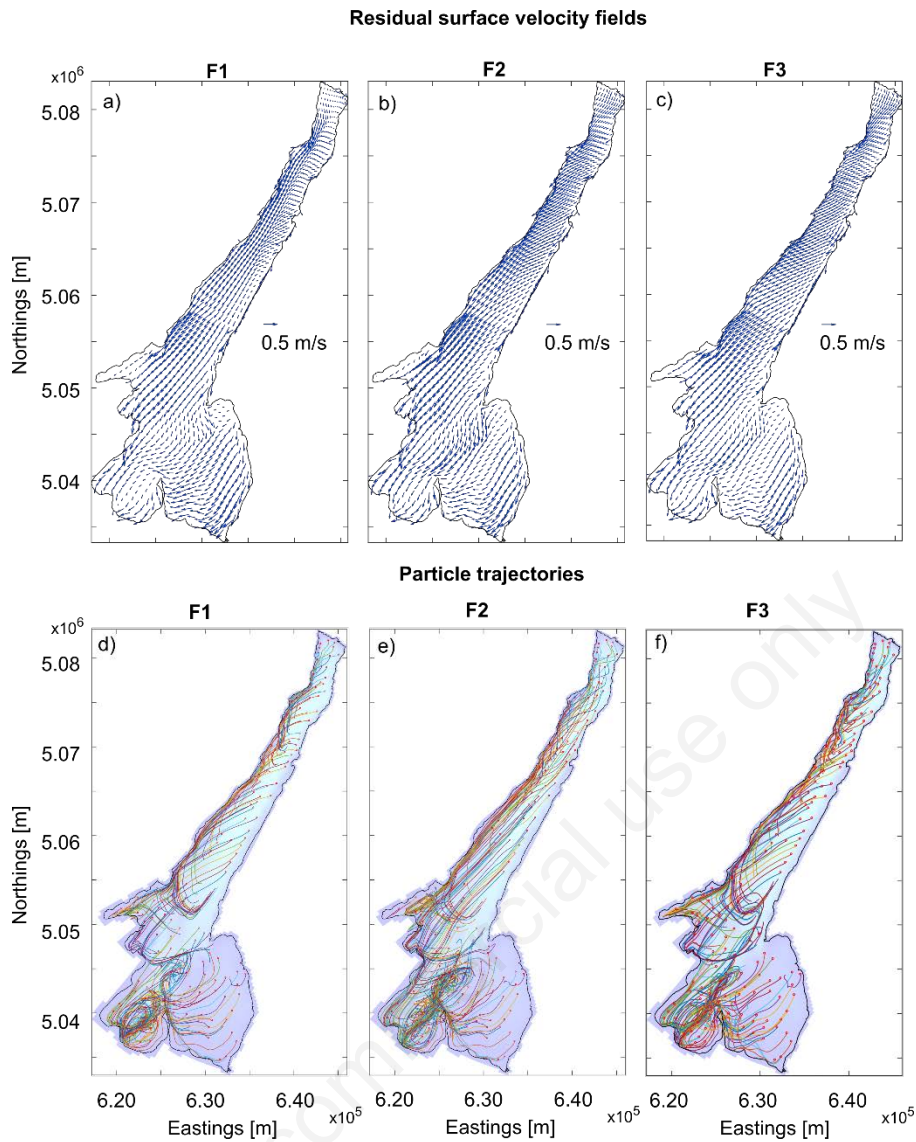


**Fig. S5.** Horizontal transport in all winter Föhn wind simulations. Top plots: residual surface currents from simulations F1 (a), F2 (b), F3 (c), obtained by an average over day 3. Bottom plots: particles trajectories after two-days Lagrangian tracking in simulations F1 (d), F2 (e), F3 (f). Particles positions are computed through an average over 100 particles in some release points and plotted at 15 minutes intervals from the release time (00:00 of hydrodynamic simulation day 3) to the end of Lagrangian simulation (24:00 of hydrodynamic simulation day 4). 60% of the total number of trajectories is plotted after a random sampling to ease the comprehension of the figure.

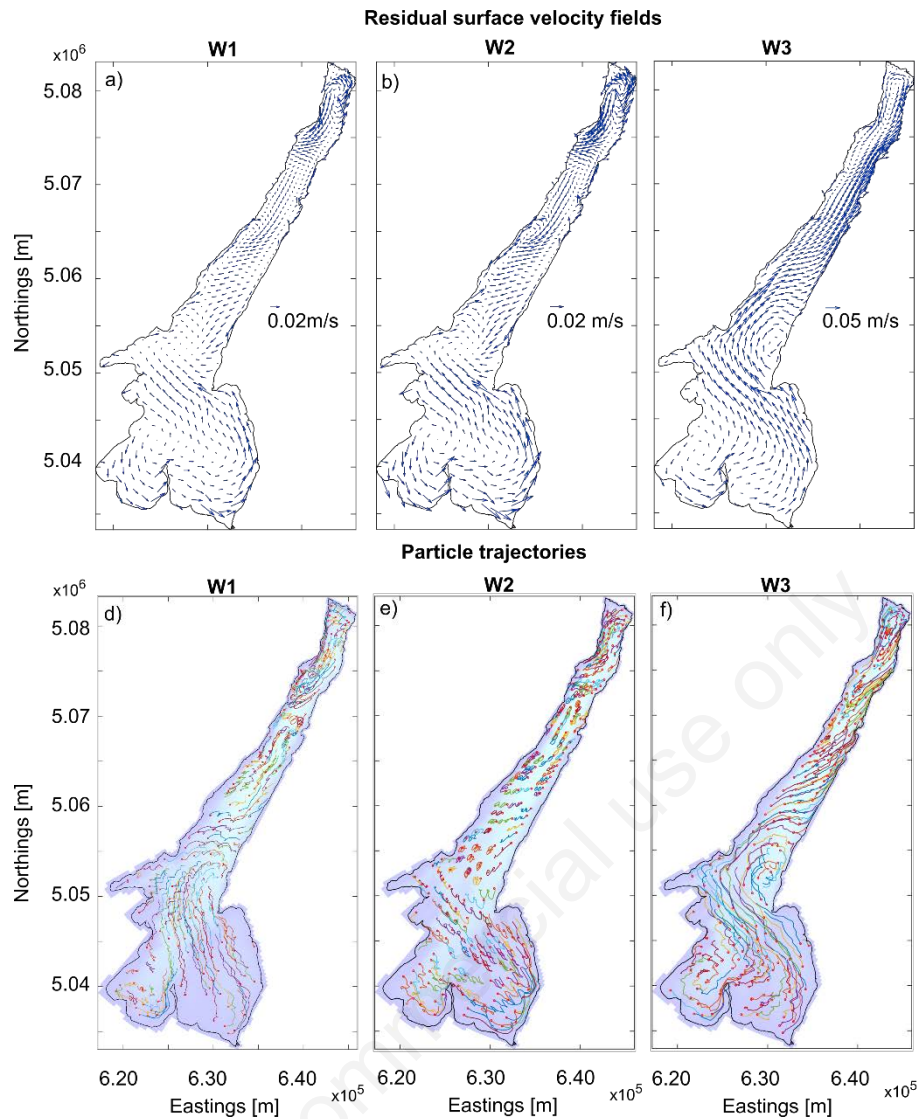


**Fig. S6.** Horizontal transport in all winter typical breeze simulations. Top plots: residual surface currents from simulations W1 (a), W2 (b), W3 (c), obtained by an average over day 3. Bottom plots: particles trajectories after two-days Lagrangian tracking in simulations W1 (d), W2 (e), W3 (f). Particles positions are computed through an average over 100 particles in some release points and plotted at 15 minutes intervals from the release time (00:00 of hydrodynamic simulation day 3) to the end of Lagrangian simulation (24:00 of hydrodynamic simulation day 4). 60% of the total number of trajectories is plotted after a random sampling to ease the comprehension of the figure.

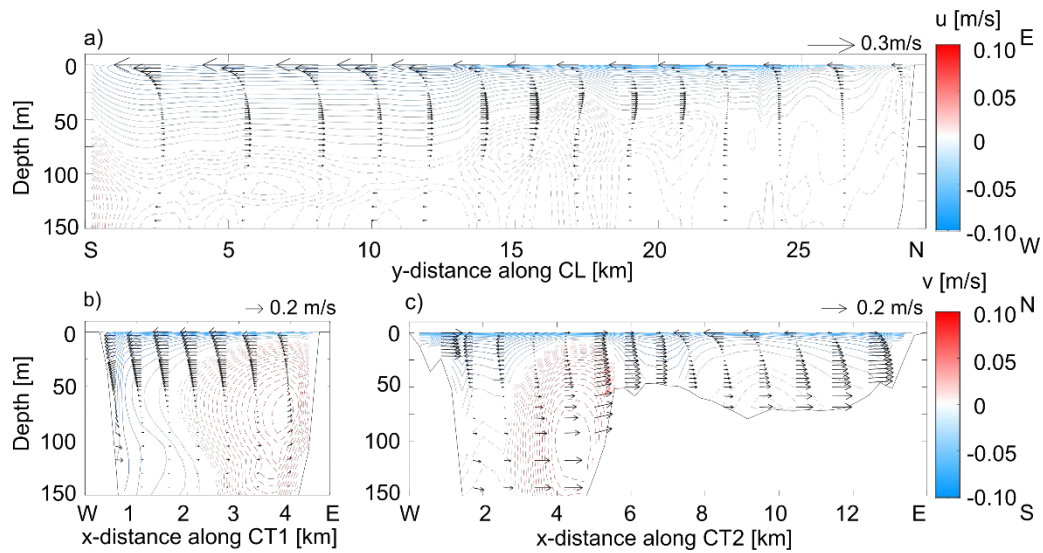


**Fig. S7.** Residual cross-section circulation from winter simulation F1, obtained by a time average over day 3: (a) longitudinal section CL, (b) northern transverse section CT1 and (c) southern transverse section CT2. The contour plot shows the magnitude of the orthogonal component of the velocity; contour lines are plotted for positive velocities, filled contour plot is for negative velocities. Arrows indicate the circulation in the section. To ease the comprehension of the figure, not all grid cells are drawn in quiver plot.

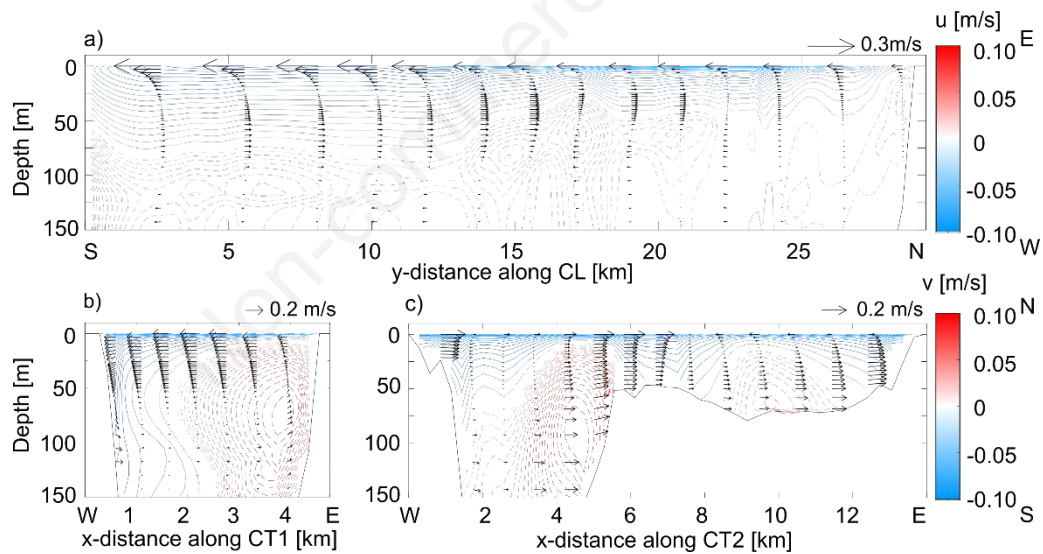


**Fig. S8.** Residual cross-section circulation from winter simulation F2, obtained by a time average over day 3: (a) longitudinal section CL, (b) northern transverse section CT1 and (c) southern transverse section CT2.

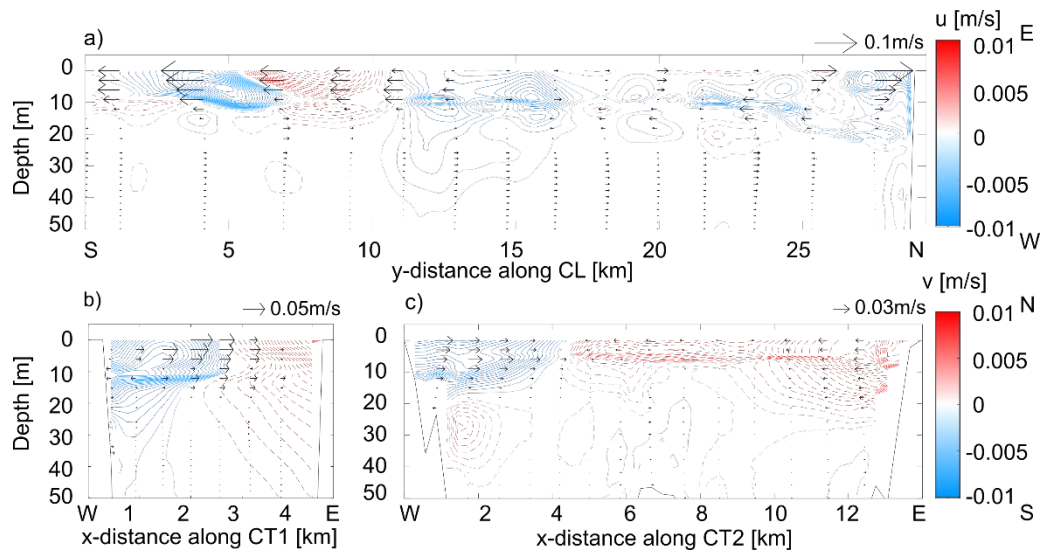


**Fig. S9.** Residual cross-section circulation from winter simulation S1, obtained by a time average over day 3: (a) longitudinal section CL, (b) northern transverse section CT1 and (c) southern transverse section CT2.

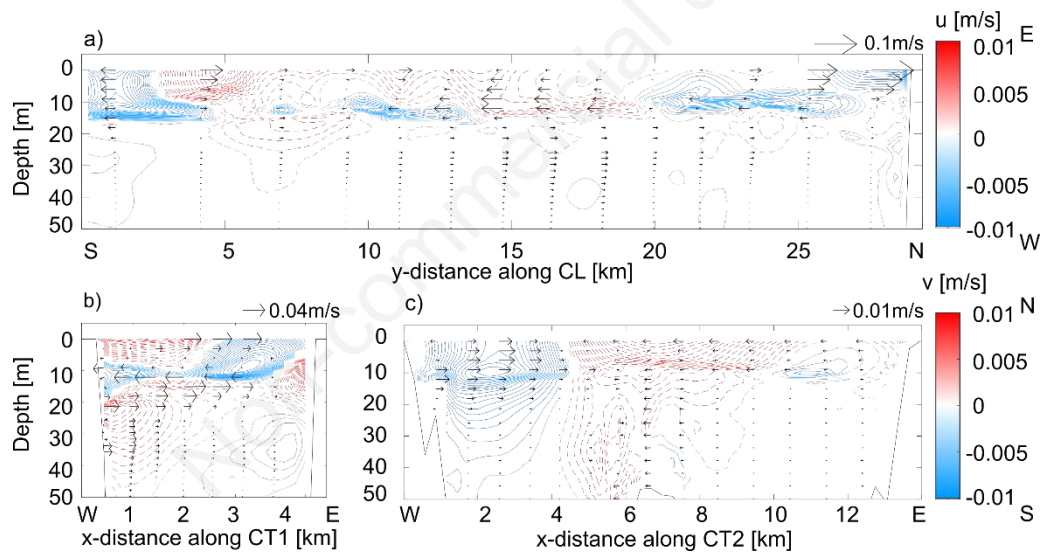


**Fig. S10.** Residual cross-section circulation from winter simulation S2, obtained by a time average over day 3: (a) longitudinal section CL, (b) northern transverse section CT1 and (c) southern transverse section CT2.

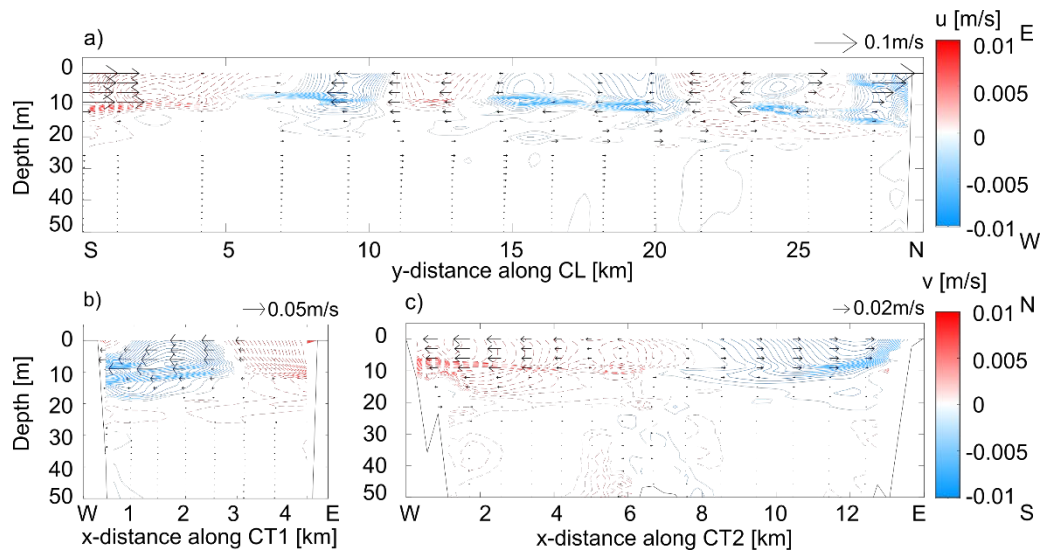


**Fig. S11.** Residual cross-section circulation from winter simulation S3, obtained by a time average over day 3: (a) longitudinal section CL, (b) northern transverse section CT1 and (c) southern transverse section CT2.

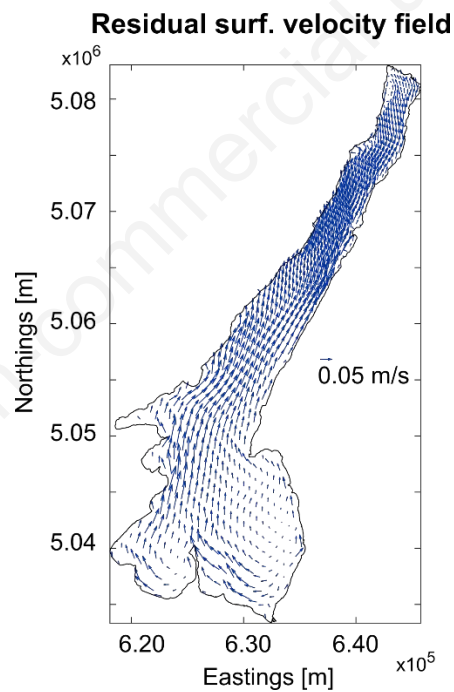


**Fig. S12.** Residual surface currents from simulations S3 performed under a uniform wind field. Wind forcing is obtained from measured data at Torbole weather station on 18th of August 2012.

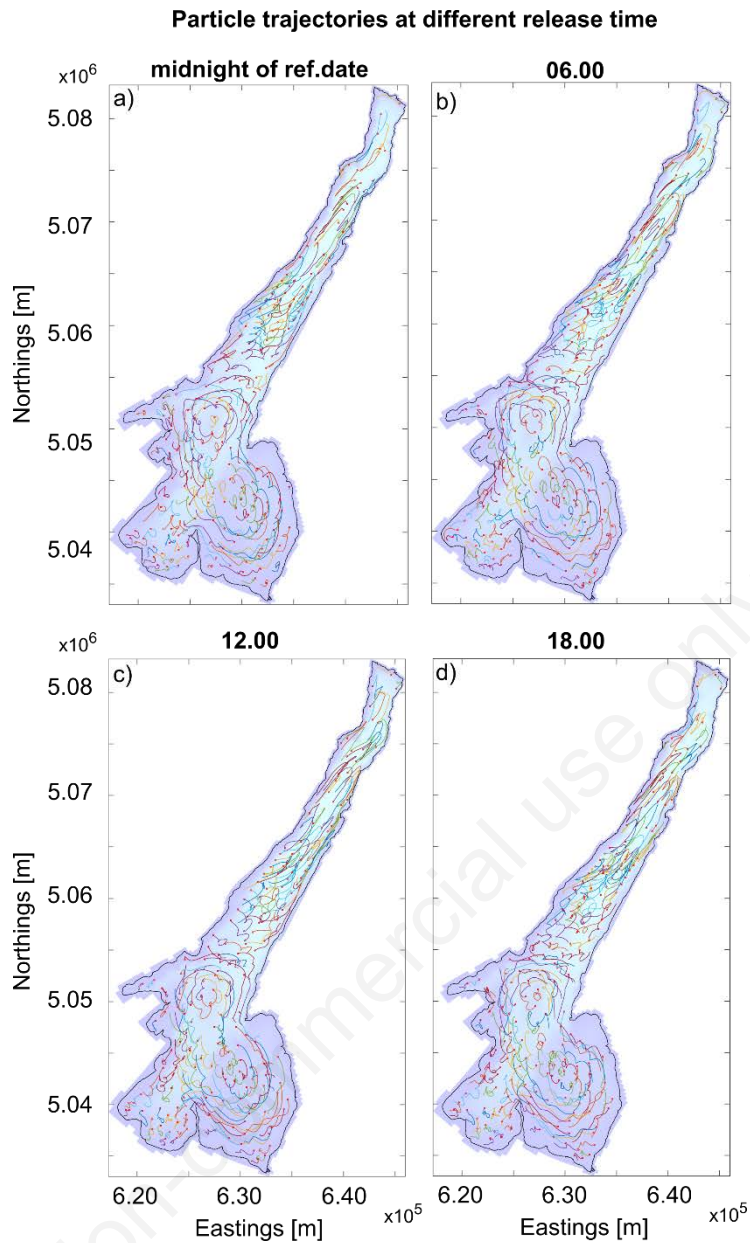


**Fig. S13.** Particles trajectories after one-day Lagrangian tracking in simulation S3 at different release time: a) at 00:00 of hydrodynamic simulation day 3; b) at 06:00 of day 3; c) at 12:00 of day 3; d) at 18:00 of day 3; at 00:00 of day 4. Particles positions are computed through an average over 100 particles in some release point and plotted at 15 minutes intervals from the release time to the end of Lagrangian simulation (24 hours later). 40% of the total number of trajectories is plotted after a random sampling to ease the comprehension of the figure.

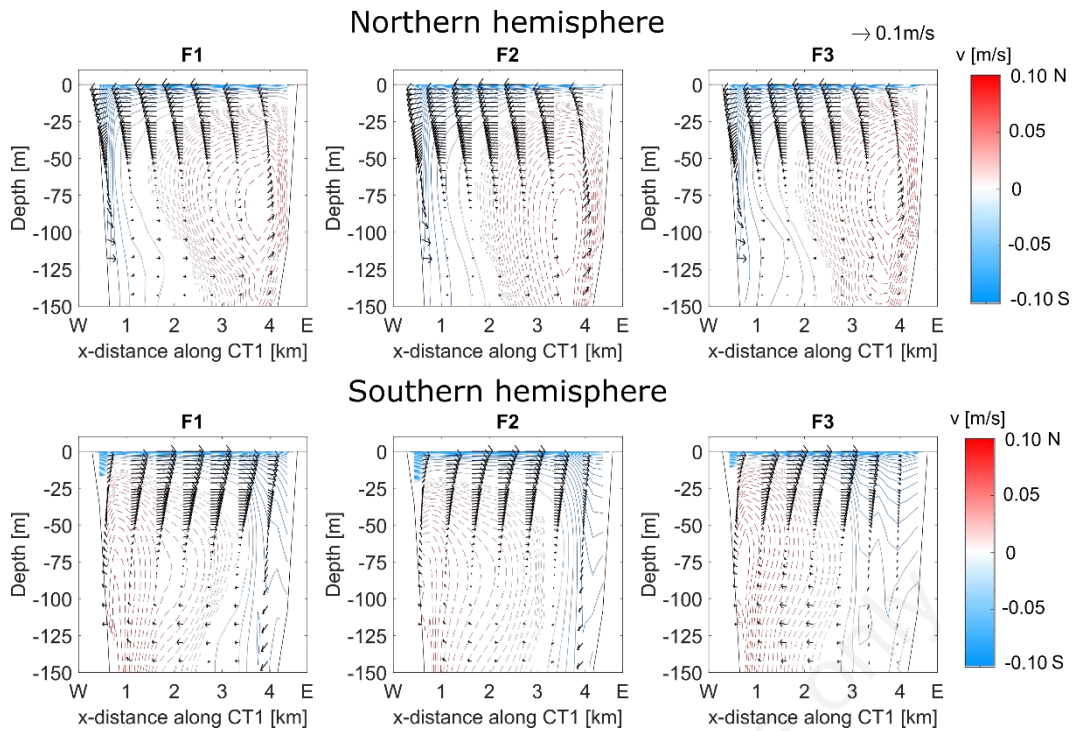


**Fig. S14.** Residual cross-section circulation in the northern transverse section CT1 from winter Föhn wind simulations performed at the real latitude (top plots, Northern hemisphere) and opposite latitude (bottom plot, Southern hemisphere), obtained by an average over the third simulated day.

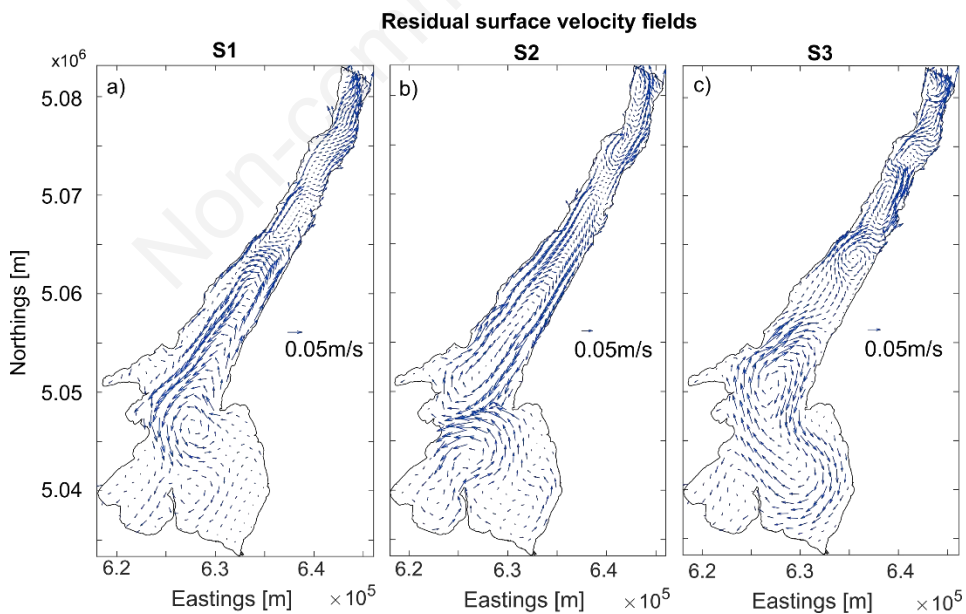


**Fig. S15.** Residual surface currents from simulations S1 (a), S2 (b), S3 (c) performed with opposite latitude (Southern hemisphere), obtained by an average over the third simulated day.

**Tab. S1.** Delft3D-FLOW parameters.

<b>Hydrodynamic simulations parameters</b>		
Simulation timestep	1 min	
Simulation time	4 days	
Number of cells in u direction	64	
Number of cells in v direction	224	
Number of layers	61	
Horizontal grid spacing	100 m – 400 m	
Vertical grid spacing	1 – 50 m	
Bottom roughness (Chézy)	$65 \text{ m}^{1/2} \text{ s}^{-1}$	(default, uniform)
Wind drag coefficient $C_d$	0.0044	$1 \text{ m s}^{-1}$
(for wind speed $W^1$ )	0.0010	$5 \text{ m s}^{-1}$
	0.0020	$10 \text{ m s}^{-1}$
Heat fluxes model	No fluxes	
Turbulence model	k- $\varepsilon$	
Horizontal eddy diffusivity	$0.2 \text{ m}^2\text{s}^{-1}$	(default, uniform)
Horizontal eddy viscosity	$0.2 \text{ m}^2\text{s}^{-1}$	(default, uniform)



**Tab. S2.** Delft3D-PART parameters.

<b>Particle tracking simulations parameters</b>		
Simulation timestep	15 min	
Simulation time	2 days	
Type of model	1	(tracer)
Instantaneous release time	00:00:00	(day 1)
Number of releases	318	
Number of particles per release	100	
Released mass	0 kg	
Release radius	10 m	
Perc. of total particles	100%	
Vertical dispersion coefficient	0 m <sup>2</sup> s <sup>-1</sup>	
Horizontal dispersion		
a parameter	0	
b parameter	0	

## REFERENCES

Wüest A, Lorke A, 2003. Small scale hydrodynamics in lakes. *Annu. Rev. Fluid Mech.* 35:373-412.